Generalized Quadrature Spatial Modulation Scheme Using Antenna Grouping

Francisco Rubén Castillo-Soria, Joaquín Cortez-González, Raymundo Ramirez-Gutierrez, Fermín Marcelo Maciel-Barboza, and Leonel Soriano-Equigua

This paper presents a novel generalized quadrature spatial modulation (GQSM) transmission scheme using antenna grouping. The proposed GQSM scheme combines QSM and conventional spatial multiplexing (SMux) techniques in order to improve the spectral efficiency (SE) of the system. Analytical and simulation results show that the proposed transmission scheme has minimal losses in terms of the average bit error probability along with the advantage of an increased SE compared with previous SM and QSM schemes. For the case studies, this advantage represents a reduction of up to 81% in terms of the number of required transmit antennas compared with QSM. In addition, a detection architecture based on the ordered successive interference cancellation scheme and the *QR* decomposition is presented. The proposed QRD-*M* adaptive algorithm showed a near-maximum-likelihood performance with a complexity reduction of approximately 90%.

Keywords: Antenna grouping, Generalized QSM, Spatial modulation.

I. Introduction

Spatial modulation (SM) is a transmission technique that is designed to work on multiple-input multiple-output (MIMO) systems [1]. In general, SM schemes exhibit advantages in terms of the bit error rate (BER) and complexity when compared to conventional spatial multiplexing (SMux) techniques such as Vertical-Bell Laboratories Layered Space-Time (V-BLAST) [2]. In addition, SM schemes are energy efficient because a reduced number of radiofrequency (RF) chains are used [3]. New research in this topic has been oriented to improve sub-optimal low-complexity detection algorithms [4]. Furthermore, some multiuser schemes that employ the SM technique have been proposed in [5]. In [6], the SM transmission technique has been considered as a key technology for future wireless communication systems. However, a major concern of SM is its suboptimal $\log_2(N_{tx})$ data-rate enhancement, while for the SMux technique, the data rate increases linearly with the number of transmit (Tx) antennas N_{tx}.

Recently, [7] proposed a transmission scheme for SM signals known as quadrature spatial modulation (QSM). The QSM scheme can be considered as a generalization of the bi-space shift keying (BiSSK) scheme proposed in [8]. It should be noted that these schemes have roughly the same BER performance as the basic SM scheme, but with the advantage of doubling the number of bits that can be transmitted in the spatial constellation, which results in an improved spectral efficiency (SE). This technique has motivated a new study that is oriented to improve the system performance while reducing the detection complexity [9], [10]. However, the number of Tx antennas required for the QSM scheme is still much higher than that required by the conventional SMux scheme, especially when high spatial constellations are considered.

Manuscript received Mar. 23, 2017; revised July 1, 2017; accepted July 19, 2017.

Francisco Rubén Castillo-Soria (corresponding author, fsoria@fc.uaslp.mx) is with the Department of Telecommunications Engineering, Autonomous University of San Luis Potosí, SLP, México.

Joaquín Cortez-González (joaquin.cortez@itson.edu.mx) is with the Electronics and Electrical Engineering Department, Technologic Institute of Sonora, México.

Raymundo Ramirez-Gutierrez (raymundo.ramirez.gutierrez@intel.com) is with the DSP and algorithms research group, Intel Labs, Guadalajara, México.

Fermin Marcelo Maciel-Barboza (fermin_maciel@ucol.mx) and Leonel Soriano-Equiga (lsoriano@ucol.mx) are with the Faculty of Mechanical and Electrical Engineering, University of Colima, Colima, México.

To overcome this drawback, this paper proposes a novel generalized QSM (GQSM) scheme based on antenna grouping. In the proposed scheme, the total number of Tx antennas N_{tx} is divided into small groups, each with two Tx antennas, in order to obtain a high SE; however, this idea can easily be extended to form groups with more than two Tx antennas. Using the principle of the QSM technique, each group transmits a different M-order quadrature amplitude modulation/phase-shift keying (M-QAM/M-PSK) symbol at each period. As a result, the proposed scheme has a significant SE improvement, which is reflected in a reduction in the total number of required Tx antennas, N_{tx}. Analytical and simulation results show that the proposed GQSM scheme using $N_{tx} = 4$ or $N_{tx} = 6$ and 4-QAM modulation requires an additional 1 dB to 2 dB in order to achieve the QSM performance; nevertheless, when $N_{tx} = 4$ and 16-QAM modulation is used, the proposed scheme shows a slightly better performance than the QSM scheme. The proposed scheme has a reduction of up to 81% over the required N_{tx} when compared to that of the reference scheme (QSM). Moreover, a low-complexity/near-maximum-likelihood (ML) architecture for the detection of GQSM signals is presented. The proposed detection architecture is based on ordered successive interference cancellation (OSIC) and the QR decomposition. The proposed QRD-M adaptive algorithm shows a near-ML performance with a complexity reduction of approximately 90%.

Throughout this paper, the following notation is used: bold and lowercase letters denote vectors, whereas bold and capital letters denote matrices. The notations $(\cdot)^T$, $(\cdot)^H$, and $\|\cdot\|$ denote the transpose, conjugate transpose, and the norm of a vector or matrix, respectively. $\mathcal{CN}(n, \sigma^2)$ is used to represent the complex Gaussian distribution of a random variable with mean n and variance σ^2. $P(\cdot)$ represents the event probability, while $E[\cdot]$ denotes the statistical expectation.

The rest of this paper is organized as follows: Section II describes in detail the proposed system and the channel model under consideration. Section III presents a theoretical analysis of ML detection for the proposed scheme. In Section IV, the complexity of the ML criterion is analyzed, while in Section V, low-complexity algorithms are proposed for the GQSM signal detection. In Section VI, the simulation results are analyzed, and conclusions are presented in Section VII.

II. System Model

1. Channel Model

It is assumed that the channel propagation between each pair of Tx and Rx antennas can be modeled as a Rayleigh narrowband stationary stochastic process. It is also considered that the channel provides rich scattering on both sides, that is, the transmitter and receiver sides. The simulation considers that a realization of the MIMO channel can be expressed as a random matrix **H** of size $N_{rx} \times N_{tx}$, where N_{tx} and N_{rx} are the number of Tx and Rx antennas, respectively. The elements of **H** are denoted by h_{ij}, for $i = 1, 2, \ldots, N_{rx}$, $j = 1, 2, \ldots, N_{tx}$. With this model, each entry of **H** at any time is a complex Gaussian random variable with zero mean and a variance of $\sigma^2/2$ per dimension. It is assumed that the temporal channel fading is slow compared with the symbol period T, where a quasi-static block-fading model is sufficient to characterize the temporal correlation. Therefore, the channel matrix **H** is randomly generated, but remains constant during the transmission of one space-time code word of length T. In addition, a perfect channel state information (CSI) is assumed at the receiver.

2. Proposed System Model

Figure 1 shows the GQSM system model, which is composed of N_{tx} and N_{rx} antennas. Let us consider small groups of two Tx antennas. Then, the GQSM system comprises $n_B = N_{tx}/2$ blocks or groups, where each group transmits one different symbol at T using the QSM technique. Let us consider an incoming data string of $n_B(\log_2(M) + 2)$ bits, where M represents the M-QAM constellation size. Considering only two Tx antennas per group, each group can transmit $m_g = 2 + \log_2(M)$ bits per channel use (bpcu). For the l-th group, the first two bits are modulated using a spatial constellation; the second $\log_2(M)$ bits are modulated using the M-QAM constellation. First, the M-QAM symbol x is divided into its real and imaginary parts: $x = x_{\Re} + jx_{\Im}$. Then, $x_{\Re}$ is transmitted using the spatial constellation in the l-th group using one Tx antenna, and $x_{\Im}$ is transmitted by another or the same Tx antenna within the same group. Each selected antenna transmits the signal $s_k^{(l)}$, $l = \{1, 2, \ldots, n_B\}$, $k = \{1, 2\}$.

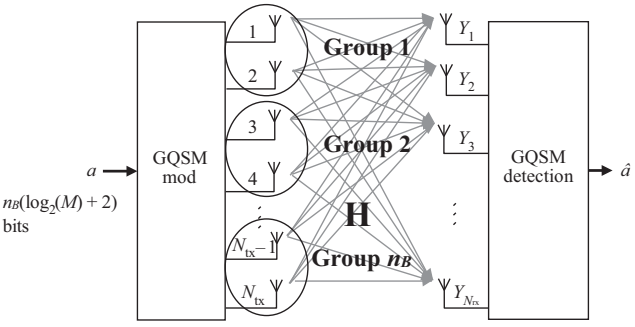

Fig. 1. GQSM system model.

https://doi.org/10.4218/etrij.17.0117.0162

The normalized transmission vector $\boldsymbol{s}^{(l)} = \left[\left(s_1^{(l)} s_2^{(l)}\right)/\sqrt{e^{(l)}}\right]$, where $l = \{1, 2, \ldots, n_B\}$ has elements $s_k^{(l)}$, which represent the signal transmitted by the l-th group and the k-th Tx antenna in the GQSM constellation. Because only two Tx antennas are used per group, the signals $s_1^{(l)}$ and $s_2^{(l)}$ are transmitted by the first and second Tx antennas, respectively. The constant $e^{(l)}$ is the normalization factor for the l-th group, which is calculated to maintain a unitary power transmission.

Table 1 shows the symbol mapping for only one group using the QPSK constellation. $A_{x\Re}$ is the antenna that transmits the real part of the M-QAM symbol, and $A_{x\Im}$ is the antenna that transmits the imaginary part. For example, in Table 1, for the input sequence a = [0000], both real and imaginary parts of the symbol (+1 +j) are transmitted by the first Tx antenna, while the second Tx antenna remains silent. A detailed explanation of the QSM scheme can be found in [8].

Consider the GQSM scheme with n_B blocks of Tx antennas (antenna grouping). The complete transmission block: $\mathbf{s}_B = [s_k^{(1)}, s_k^{(2)}, \ldots, s_k^{(n_B)}]/\sqrt{n_B}$ is composed of a concatenated output of all groups. The transmission vector $\mathbf{s}_B$ is conveyed over the random complex wireless channel $\mathbf{H}$ defined in Section II-1. For simplicity, it is assumed that all of the Tx antennas convey information symbols from the same constellation map; it is also assumed that the receiver is perfectly synchronized. The number of bpcu that can be transmitted for the complete transmission vector $\mathbf{s}_B$ in the proposed GQSM scheme is $m_{\text{GQSM}} = n_B(\log_2(M) + 2) = N_{\text{tx}}(\log_2(\sqrt{M}) + 1)$bpcu. The number of bits that can be transmitted using QSM is $m_{\text{QSM}} = \log_2(M) + 2\log_2(N_{\text{tx}})$ bpcu [8]. The number of bits that can be transmitted using SM is $m_{\text{SM}} = \log_2(M) + \log_2(N_{\text{tx}})$ [1]. The number of bits that can be transmitted using SMux is $m_{\text{SMux}} = N_{\text{tx}}\log_2(M)$ [2]. Figure 2 shows a comparison of the SE in bpcu for SM, QSM, GQSM, and SMux transmission schemes for different configurations. For the proposed GQSM scheme, the improvement in the SE can be seen in terms of the required number of Tx antennas. For example, considering a transmission of 8 bpcu and 4-QAM, the proposed GQSM scheme requires four Tx antennas, the GSM scheme proposed in [11] requires at least eight Tx antennas, and the SM-SMux scheme [12] requires at least four Tx antennas.

At the receiver, the CSI and σ_n^2 are assumed to be known. In addition, it is assumed that $\mathbf{H}$ is full-rank. During every T, the sequence of symbols $s_k^{(l)}$ is transmitted and multiplexed over the N_{tx} antennas. Therefore, the system equation can be expressed as

$$\begin{bmatrix} y_1 \\ \vdots \\ y_{N_{\text{rx}}} \end{bmatrix} = \begin{bmatrix} h_{1,1} & \cdots & h_{1,N_{\text{tx}}} \\ \vdots & \ddots & \vdots \\ h_{N_{\text{rx}},1} & \cdots & h_{N_{\text{rx}},N_{\text{tx}}} \end{bmatrix} \begin{bmatrix} s_1^{(1)} \\ \vdots \\ s_k^{(n_B)} \end{bmatrix} + \begin{bmatrix} n_1 \\ \vdots \\ n_{N_{\text{rx}}} \end{bmatrix}, \quad (1)$$

or equivalently,

$$\boldsymbol{y} = \sqrt{\rho}\mathbf{H}\mathbf{s}_B + \boldsymbol{n}, \quad (2)$$

where $\boldsymbol{y}$ is the received signal vector, ρ is the signal-to-noise-ratio (SNR) at the receiver, $h_{i,j}$. is the channel gain for $i = 1, 2, \ldots, N_{\text{rx}}$ and $j = 1, 2, \ldots, N_{\text{tx}}$, and n is the noise vector at the receiver. The noise samples n_i are

Table 1. GQSM constellation for 4-QAM and two Tx antennas.

$a = [a_1\ a_2\ a_3\ a_4]$	$(A_{x\Re}, A_{x\Im})$, QPSK symbol	$S_1^{(l)} S_2^{(l)}$
[0 0 0 0]	[(1, 1), (+1 + j)]	[1 + j, 0]
[0 0 0 1]	[(1, 1), (−1 + j)]	[−1 + j, 0]
[0 0 1 0]	[(1, 1), (+1 − j)]	[1 − j, 0]
[0 0 1 1]	[(1, 1), (−1 − j)]	[−1 − j, 0]
[0 1 0 0]	[(1, 2), (+1 + j)]	[1, j]
[0 1 0 1]	[(1, 2), (−1 + j)]	[−1, j]
[0 1 1 0]	[(1, 2), (+1 − j)]	[1, −j]
[0 1 1 1]	[(1, 2), (−1 − j)]	[−1, −j]
[1 0 0 0]	[(2, 1), (+1 + j)]	[j, 1]
[1 0 0 1]	[(2, 1), (−1 + j)]	[j, −1]
[1 0 1 0]	[(2, 1), (+1 − j)]	[−j, 1]
[1 0 1 1]	[(2, 1), (−1 − j)]	[−j, −1]
[1 1 0 0]	[(2, 2), (+1 + j)]	[0, 1 + j]
[1 1 0 1]	[(2, 2), (−1 + j)]	[0, −1 + j]
[1 1 1 0]	[(2, 2), (+1 − j)]	[0, 1 − j]
[1 1 1 1]	[(2, 2), (−1 − j)]	[0, −1 − j]

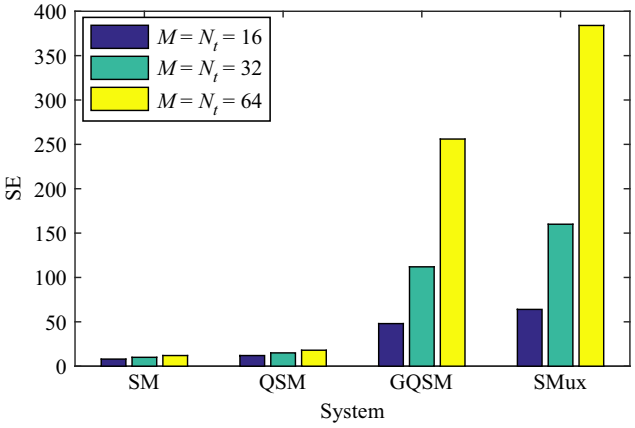

Fig. 2. Comparison of spectral efficiency in bpcu.

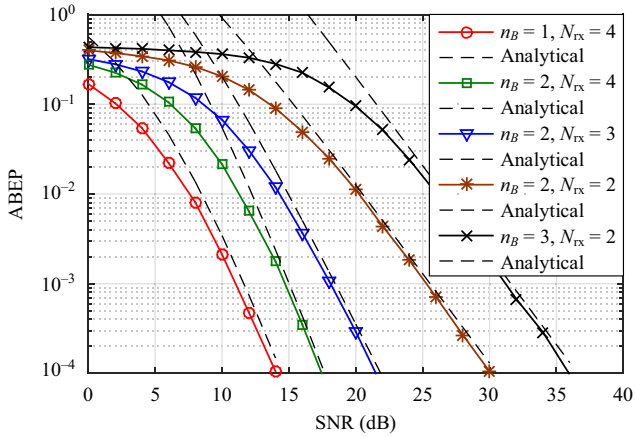

Fig. 3. Analytical and simulation results of the GQSM scheme utilizing the ML criterion and 4-QAM.

independent identically distributed (i.i.d.) complex Gaussian random variables with CN(0, σ_n^2).

At the receiver, the signals of all groups are detected at the same time. The optimal detection for GQSM signals is given by the ML criterion, which is defined as

$$[\hat{\boldsymbol{s}}_B] = \arg\min_{S} \|\boldsymbol{y} - \sqrt{\rho}\mathbf{H}\mathbf{s}_B\|_F^2. \quad (3)$$

Finally, the original sequence of bits can be detected by employing the mapping rule used for $\mathbf{s}_B$.

III. Average Bit Error Probability Derivation

The average bit error probability (ABEP) can be derived by using the well-known bounding technique. Considering that $g_i = \sqrt{\rho}\mathbf{H}\mathbf{s}_B$, the probability of deciding on $\hat{g}_j$ given that g_i is transmitted is upper bounded as

$$P_s = E\left[\cup_j P(g_i \to \hat{g}_j)\right] \le \sum\nolimits_j P(g_i \to \hat{g}_j), \quad (4)$$

where $E[\cdot]$ represents the expected value and $P(g_i \to \hat{g}_j)$ is the pairwise error probability (PEP) of deciding on the signal $\hat{g}_j$ given that g_i is transmitted. The conditional PEP can be calculated as

$$P(g_i \to \hat{g}_j|\mathbf{H}) = Q(\sqrt{v}), \quad (5)$$

where $Q[\cdot]$ is the Q function, which is defined as $Q(x) = \frac{1}{\sqrt{2\pi}}\int_x^\infty e^{\frac{-t^2}{2}}dt$, and $v = 3\rho/(N_{rx} + 5)$. Considering a probability density function $p(v)$, the total PEP for the fading channel can be calculated using the mathematical expectation as follows:

$$P(g_i \to \hat{g}_j) = E\left[P(g_i \to \hat{g}_j|\mathbf{H})\right] = \int_{v=0}^{\infty} Q(\sqrt{v})p(v)dv. \quad (6)$$

Considering a single Rx antenna, the probability of error can be solved as [7]

$$P(g_i \to \hat{g}_j) = \frac{1}{2}\left(1 - \sqrt{\frac{v}{1+v}}\right). \quad (7)$$

If the receiver is equipped with $N_{rx} > 1$ Rx antennas, $P(g_i \to \hat{g}_j) = Q(\sqrt{\sum_{k=1}^{N_{rx}} v_k})$, which has a closed-form expression that is obtained as

$$P(g_i \to \hat{g}_j) = \gamma^{N_{rx}} \sum_{k=0}^{N_{rx}-1} \binom{N_{rx} - 1 + k}{k} [1-\gamma]^k, \quad (8)$$

where γ is the PEP for a single Rx antenna [13]. Using (4), the ABEP for a general GQSM scheme can be computed as

$$P_{e,\text{GQSM}} \le [MM']^{(n_B-1)} \sum_{i=1}^{MM'} \sum_{j=1}^{MM'} \frac{N(i,j)P(g_i \to \hat{g}_j)}{MM'\text{Log}_2(MM')}, \quad (9)$$

where $N(i, j)$ is the number of bits in error associated with the corresponding PEP, and M' is the spatial constellation size. Note that if $n_B = 1$, the ABEP for QSM is obtained.

Substituting (8) into (9) and considering a spatial constellation of size $M' = 4$ (groups of two Tx antennas), the ABEP for the proposed GQSM scheme can be computed as

$$P_{e,\text{GQSM}} \le [4M]^{(n_B-1)} \sum_{i=1}^{4M} \sum_{j=1}^{4M} \frac{N(i,j)\gamma^{N_{rx}} \sum_{k=0}^{N_{rx}-1} \binom{N_{rx} - 1 + k}{k} [1-\gamma]^k}{4M(\log_2(M) + 2)}. \quad (10)$$

Figure 3 illustrates the analytical upper bound in (10) using the ML criterion and 4-QAM for different configurations of n_B and N_{rx}.

IV. Complexity

The receiver complexity η for the ML criterion in (3) is measured in terms of complex operations (CO). One arithmetic operation is considered as one CO, and one comparison is considered as one CO. The lattice in the system has 2^m points. After performing subtraction, obtaining the square, and finding the minimum in (3), the result obtained is $(3 + D)2^m$ CO. Considering N_{rx} Rx antennas, the complexity of the ML in (3) can be approximated by

$$\eta \approx (3 + D)N_{rx}2^m, \quad (11)$$

where m is the number of bpcu for each system defined in Section I, and D is a factor that depends on the number of

Table 2. Complexity comparison for the ML criterion in CO.

Transmission scheme	8 bpcu (4-QAM) $N_{rx} = 4$	12 bpcu (16-QAM) $N_{rx} = 4$	12 bpcu (4-QAM) $N_{rx} = 6$
SM	4,096	65,536	98,304
QSM	4,096	65,536	98,304
GQSM	5,120	81,920	147,456
SMux	10,240	163,840	344,064

COsx that are required to generate one symbol in the constellation in (3). The SM scheme requires only one multiplication ($D = 1$), and QSM requires two multiplications, but with only one QAM symbol ($D = 1$), GQSM requires a combination of n_B groups ($D = n_B = N_{tx}/2$ CO), and SMux requires that all transmitted signals be combined ($D = 2N_{tx} - 1$). This result shows that the complexity of the proposed scheme is between that of QSM and SMux, and that it depends on n_B. Table 2 shows a comparison of the complexity for ML detection considering the three case studies.

V. Low-Complexity Detection Algorithms for GQSM Signals

The ML criterion is the optimal detector; however, its high complexity may be restrictive for real implementations. To overcome this drawback, in this section, two different detection algorithms are proposed for the GQSM scheme. Both algorithms follow three similar steps, where the system equations are rewritten to obtain a more convenient representation, the *QR* decomposition of $\mathbf{H}$ is carried out, and the decoding problem is set as a search tree.

Using OSIC techniques based on the zero-forcing (ZF) solution in V-BLAST systems, the order of detection is very important because an optimum order can reduce the risk of error propagation in the estimation of the transmitted symbols. Reference [14] proposes a very efficient method to obtain an optimal order based on the minimum mean-square error (MMSE) sorted *QR* decomposition of $\mathbf{H}$. The algorithm is presented as an extension to the modified Gram-Schmidt (MGS) algorithm [15] by reordering the blocks of the GQSM system, and this is done by reordering the columns of the channel matrix prior to each orthogonalization step. Reordering the channel matrix $\mathbf{H}$ results in matrix $\underline{\mathbf{R}}$, with rows sorted from the highest to the lowest SNR [14]. In order to reduce the complexity of the *QR* decomposition process, the norm pre-computing of columns in the matrix $\underline{\mathbf{Q}}$ was introduced and updated according to the MGS algorithm proposed in [16]. The complete MMSE SQRD-GQSM algorithm is shown in Table 3.

1. OSIC-MMSE Sorted *QR* Decomposition Detector for GQSM Scheme (OSIC MMSE SQRD – GQSM)

In order to extend the *QR*-based detection with respect to the MMSE criterion, the *QR* decomposition is carried out for the extended $\underline{\mathbf{H}}$, which is defined as:

$$\underline{\mathbf{H}} = \begin{bmatrix} H \\ \sigma_n \mathbf{I}_{N_{tx}} \end{bmatrix} = \underline{\mathbf{Q}}\underline{\mathbf{R}} = \begin{bmatrix} \mathbf{Q}_1 \\ \mathbf{Q}_2 \end{bmatrix} \underline{\mathbf{R}} = \begin{bmatrix} \mathbf{Q}_1 \underline{\mathbf{R}} \\ \mathbf{Q}_2 \underline{\mathbf{R}} \end{bmatrix}, \quad (12)$$

where the $(N_{tx} + N_{rx}) \times N_{tx}$ matrix $\underline{\mathbf{Q}}$ with orthonormal columns is partitioned into $(N_{rx} \times N_{tx})$ matrix $\mathbf{Q}_1$ and $(N_{tx} \times N_{tx})$ matrix $\mathbf{Q}_2$, with $(N_{rx} \times N_{tx})$ matrix $\underline{\mathbf{Q}}$.

The algorithm proposed in [14] (see Table 3) was modified in order to implement the OSIC process in the detection of the GQSM scheme. After calculation of the

Table 3. MMSE SQRD-GQSM algorithm.

(1) $\underline{\mathbf{R}} = 0$, $\underline{\mathbf{Q}} = \mathbf{H}$, ***order*** $= 1{:}1{:}n_B$, $ind = 1$
(2) **for** $i = 1, \ldots, N_{tx}$
(3) $\quad$ ***normb***$_i = \|\boldsymbol{q}_i\|^2$
(4) **end for**
(5) $index = 1$
(6) **for** $i = 1, \ldots, N_{tx}$
(7) $\quad$ if(mod(i, 2) $\neq$ 0)
(8) $\quad\quad$ [*ind block*] $= \arg^{\min}_{l=i:2:N_{tx}}$ (***normb***$_l$)
(9) $\quad\quad$ exchange columns i and $i + 1$
$\quad\quad$ for *ind* and *ind* + 1 in $\underline{\mathbf{R}}$, ***normb***
$\quad\quad$ and in the first $N_r + i - 1$ rows of $\underline{\mathbf{Q}}$
$\quad\quad$ exchange columns *index* and *block* of ***order***
$\quad\quad$ *index* = *index* + 1
(10) $\quad$ end
(11) $r_{i,i} = \|\boldsymbol{q}_i\|^2$
(12) $\boldsymbol{q}_i = \boldsymbol{q}_i / r_{i,i}$
(13) $\quad$ **for** $k = i + 1, \ldots, N_{tx}$
(14) $\quad\quad$ $r_{i,k} = \boldsymbol{q}_i^H \boldsymbol{q}_k$
(15) $\quad\quad$ $\boldsymbol{q}_k = \boldsymbol{q}_k - r_{i,k} \cdot \boldsymbol{q}_i$
(16) $\quad\quad$ ***normb***$_k$ = ***normb***$_k - |r_{i,k}|^2$
(17) $\quad$ **end for**
(18) **end for**

MMSE SQRD-GQSM decomposition for the channel matrix $\underline{\mathbf{H}}$, that is, $\underline{\mathbf{H}} = \underline{\mathbf{Q}}\underline{\mathbf{R}} = \begin{bmatrix} \mathbf{Q}_1 \\ \mathbf{Q}_2 \end{bmatrix} \underline{\mathbf{R}}$, where $\mathbf{Q}_1$ is a unitary matrix and $\underline{\mathbf{R}}$ is an upper triangular matrix. By multiplying the received signal in (2) by $\underline{\mathbf{Q}}_1^H$, the modified received vector is

$$\tilde{\boldsymbol{y}} = \underline{\mathbf{Q}}_1^H \boldsymbol{y} = \underline{\mathbf{R}}\boldsymbol{s}_{\mathrm{GQSM}} + \mathbf{Q}_1^H \boldsymbol{n}, \tag{13}$$

if vector $\boldsymbol{s}_{\mathrm{GQSM}}$ is transmitted. Note that the statistical properties of the noise $\tilde{\boldsymbol{n}} = \mathbf{Q}_1^H \boldsymbol{n}$ remain unchanged.

The OSIC block detector was proposed considering the GQSM constellation for one block of two Tx antennas. The constellation ω_{GQSM} has a size of $2^{m_{\mathrm{GQSM}}}$ (see Table 1); therefore, it is possible to achieve a complexity reduction with respect to the ML detector. Then, it is necessary to rewrite (1) as a block system

$$\begin{bmatrix} \tilde{\boldsymbol{y}}_1 \\ \vdots \\ \tilde{\boldsymbol{y}}_{n_B} \end{bmatrix} = \begin{bmatrix} \underline{\mathbf{R}}_{11} & \cdots & \underline{\mathbf{R}}_{1n_B} \\ \vdots & \ddots & \vdots \\ 0 & \cdots & \underline{\mathbf{R}}_{n_B n_B} \end{bmatrix} \begin{bmatrix} \boldsymbol{s}_1 \\ \vdots \\ \boldsymbol{s}_{n_B} \end{bmatrix} + \begin{bmatrix} \tilde{\boldsymbol{n}}_1 \\ \vdots \\ \tilde{\boldsymbol{n}}_{n_B} \end{bmatrix}, \tag{14}$$

which can be expressed as a matrix equation

$$\tilde{\boldsymbol{y}}_B = \underline{\mathbf{R}}_B \boldsymbol{s}_B + \tilde{\boldsymbol{n}}_B, \tag{15}$$

where block matrix $\underline{\mathbf{R}}_B \in C^{N_{\mathrm{tx}} \times N_{\mathrm{tx}}}$ is called a block matrix GQSM, and each block of $\underline{\mathbf{R}}_B$ is given by

$$\underline{\mathbf{R}}_{km} = \begin{bmatrix} \underline{r}_{2k-1,2k-1} & \underline{r}_{2k-1,2k} \\ 0 & \underline{r}_{2k,2k} \end{bmatrix}, \tag{16}$$

for $m = 1, 2, \ldots, n_B$, $k = 1, 2, \ldots, n_B$, and $m = k$. In the case with $m > k$, $\underline{\mathbf{R}}_B$ is given by

$$\underline{\mathbf{R}}_{km} = \begin{bmatrix} \underline{r}_{2k-1,2m-1} & \underline{r}_{2k-1,2m} \\ \underline{r}_{2k,2m-1} & \underline{r}_{2k,2m} \end{bmatrix}. \tag{17}$$

Now, each block of $\tilde{\boldsymbol{y}}_k$, $\tilde{\boldsymbol{s}}_k$, and $\tilde{\boldsymbol{n}}_k$ for $k = 1, 2, \ldots, n_B$ is

$$\tilde{\boldsymbol{y}}_k = \begin{bmatrix} \tilde{y}_{2k-1} \\ \tilde{y}_{2k} \end{bmatrix}, \tilde{\boldsymbol{s}}_k = \begin{bmatrix} \tilde{s}_{2k-1} \\ \tilde{s}_{2k} \end{bmatrix}, \tilde{\boldsymbol{n}}_k = \begin{bmatrix} \tilde{n}_{2k-1} \\ \tilde{n}_{2k} \end{bmatrix}. \tag{18}$$

Owing to the upper block triangular structure of $\underline{\mathbf{R}}_B$, the k-th element of $\tilde{\boldsymbol{y}}$ is

$$\tilde{\boldsymbol{y}}_k = \tilde{\mathbf{R}}_{kk}\tilde{\boldsymbol{s}}_k + \sum_{i=k+1}^{n_B} \tilde{\mathbf{R}}_{ki}\tilde{\boldsymbol{s}}_i + \tilde{\boldsymbol{n}}_k. \tag{19}$$

The blocks are estimated in sequence, from the lower to the higher stream, using OSIC. Assuming that all previous block decisions are correct, the interference can be perfectly cancelled at each step except for the additive noise. The estimated vector $\hat{\boldsymbol{s}}_k$ is given by

$$\hat{\boldsymbol{s}}_k = D\left[\frac{\tilde{\boldsymbol{y}}_k - \sum_{i=k+1}^{n_B} \tilde{\mathbf{R}}_{ki}\hat{\boldsymbol{s}}_i}{\tilde{\mathbf{R}}_{kk}}\right], \tag{20}$$

where $\hat{\boldsymbol{s}}_k$ is the estimate of s_k and $D(\cdot)$ is a decision device that maps its argument to the closest signal in the GQSM constellation. A full description of the OSIC detector is shown in Table 4.

The algorithms were written using MATLAB notation. Variables in bold represent either vectors (lowercase) or matrices (uppercase). Vector and matrix indexing are indicated using square brackets. $\boldsymbol{\Omega}_{\mathrm{GQSM}}$ is a matrix whose rows elements are the GQSM constellation symbols.

2. Near-ML MMSE Sorted *QR* Decomposition for GQSM Scheme (Near-ML MMSE SQRD – GQSM)

In this section, the advantages of combining QRM-algorithm [17] and the sphere detector (SD) [18] with MMSE-sorted QR decomposition are presented. In the proposed approach, a search was carried out in breadth-first (QRM algorithm), after which a depth-first search tree algorithm based on SD was used. As a result, a similar performance in terms of BER compared to that

Table 4. OSIC MMSE SQRD-GQSM.

(1)	INPUT: $\underline{\mathbf{R}}$, $\mathbf{Q}_1$, $\boldsymbol{y}$, $\boldsymbol{\Omega}_{\mathrm{GQSM}}$, ***order***, n_B
(2)	OUTPUT: $\hat{\boldsymbol{s}}_{\mathrm{GQSM}}$
(3)	$\tilde{\boldsymbol{y}} = \mathbf{Q}_1^H \boldsymbol{y}$
(4)	$d_t = 0$
(5)	**for** $k = n_B$:−1:1
(6)	Calculate and sort the metrics $\mathbf{D}_{nB}^2 = \lVert\tilde{\boldsymbol{y}}_{nB} - \underline{\mathbf{R}}_{nBnB}\boldsymbol{x}_{nB}\rVert^2$ of value in ascending order with its corresponding position, for all possible values of $\boldsymbol{x}_{nB} \in \boldsymbol{\Omega}_{\mathrm{GQSM}}$. Store the values in **dist** and **ord,** respectively.
(7)	$\hat{\boldsymbol{x}}_{nB} = \boldsymbol{\Omega}_{\mathrm{GQSM}}(\mathbf{ord}(1),:)$
(8)	$d_t = d_t + \mathbf{dist}(1)$
(9)	**for** $m = k - 1$:−1:1
(10)	$\tilde{\boldsymbol{y}}_m = \tilde{\boldsymbol{y}}_m - \underline{\mathbf{R}}_{mk} * \hat{\boldsymbol{x}}_{nB}$
(11)	**end for**
(12)	$\hat{\boldsymbol{s}}_{\mathrm{GQSM}}(k) = \hat{\boldsymbol{x}}_{nB}$
(13)	**end for**
(14)	permutate $\hat{\boldsymbol{s}}_{\mathrm{GQSM}}$ according ***order***
(15)	**return** $\hat{\boldsymbol{s}}_{\mathrm{GQSM}}$

https://doi.org/10.4218/etrij.17.0117.0162

of the ML criterion is obtained, with an important reduction in the detection's complexity. In this work, the GQSM scheme with $n_B = 2$ and three blocks was considered. The near-ML detector operates for $N_{rx} \geq N_{tx}/2$. The aim of the near-ML detector is to find the optimum solution to the ML in (3) using the distances calculated during the process to find the closest vector in (20). For clarity, the next metric to select the estimated symbol vector $\hat{\boldsymbol{s}}_{\mathrm{GQSM}}$ is defined as

$$\hat{\boldsymbol{s}}_{\mathrm{GQSM}} = \arg \min_{x \in \boldsymbol{\Omega}_{GQSM}} \sum_{i=1}^{n_B} \mathbf{D}_i^2, \tag{21}$$

where $\mathbf{D}_i^2$ with $n_B = 2$ are given by

$$\mathbf{D}_1^2 = \|\tilde{\boldsymbol{y}}_1 - \underline{\mathbf{R}}_{11} x_1 - \underline{\mathbf{R}}_{12} x_2\|^2, \tag{22}$$

$$\mathbf{D}_2^2 = \|\tilde{\boldsymbol{y}}_2 - \underline{\mathbf{R}}_{22} \boldsymbol{x}_2\|^2, \tag{23}$$

and $\mathbf{D}_i^2$ with $n_B = 3$ are given by

$$\mathbf{D}_1^2 = \|\tilde{\boldsymbol{y}}_1 - \underline{\mathbf{R}}_{11} \boldsymbol{x}_1 - \underline{\mathbf{R}}_{12} \boldsymbol{x}_2 - \underline{\mathbf{R}}_{13} \boldsymbol{x}_3\|^2, \tag{24}$$

$$\mathbf{D}_2^2 = \|\tilde{\boldsymbol{y}}_2 - \underline{\mathbf{R}}_{22} \boldsymbol{x}_2 - \underline{\mathbf{R}}_{23} x_3\|^2, \tag{25}$$

$$\mathbf{D}_3^2 = \|\tilde{\boldsymbol{y}}_3 - \underline{\mathbf{R}}_{33} \boldsymbol{x}_3\|^2, \tag{26}$$

$$\mathbf{D}_T^2 = \sum_{i=1}^{n_B} \mathbf{D}_i^2, \tag{27}$$

where $\boldsymbol{x}_i \in \boldsymbol{\Omega}_{\mathrm{GQSM}}$ is a vector that contains all of the psible constellation symbols. Consider a breadth-first tree search. The full description of the near-ML detection algorithm for $n_B = 3$ is shown in Table 5.

However, this procedure can be improved in several ways. First, the iteration between step 5 and step 32 does not need to be over all vectors $\hat{\boldsymbol{x}}_1$, $\hat{\boldsymbol{x}}_2$, and $\hat{\boldsymbol{x}}_3$. Because the vectors are sorted in order of increasing distance, the likelihood of vectors $(\hat{\boldsymbol{x}}_1, \hat{\boldsymbol{x}}_2, \hat{\boldsymbol{x}}_3)$ being in the optimal solution decreases as the algorithm progresses, mainly for high SNRs. This suggests that some pairs of vectors may be skipped, and that the search can be stopped early according to some criterion, resulting in a significant reduction in complexity. The criterion should maximize the probability of the optimum solution, which has to be included in the search, while minimizing the number of vector pairs that are examined. This is the main reason for which the algorithm improves the complexity. The algorithm for $n_B = 2$ can be easily obtained by making minimal changes to this pseudo code.

Table 5. Near-ML MMSE SQRD-GQSM detector for $n_B = 3$.

(1)	INPUT: $\underline{\mathbf{R}}$, $\mathbf{Q}_1$, $\boldsymbol{y}$, $\boldsymbol{\Omega}_{\mathrm{GQSM}}$, ***order***, N_c = length ($\boldsymbol{\Omega}_{\mathrm{GQSM}}$)
(2)	OUTPUT: $\hat{\boldsymbol{s}}_{\mathrm{GQSM}}$
(3)	$\tilde{\boldsymbol{y}} = \boldsymbol{Q}_1^H \boldsymbol{y}$
(4)	Compute and sort the metrics $\mathbf{D}_3^2 = \|\tilde{\boldsymbol{y}}_3 - \underline{\mathbf{R}}_{33} \boldsymbol{x}_3\|^2$ in ascending order with its corresponding position, for all possible values of $\boldsymbol{x}_3 \in \boldsymbol{\Omega}_{\mathrm{GQSM}}$. Store the values in **dist3** and **ord3,** respectively.
(5)	$D = \infty$;
(6)	**for** $k = 1: N_c$,
(7)	$\hat{\boldsymbol{x}}_3 = \boldsymbol{\Omega}_{\mathrm{GQSM}}(\mathbf{ord3}(k),:)$
(8)	Compute and sort the metrics $\mathbf{D}_2^2 = \|\tilde{\boldsymbol{y}}_2 - \underline{\mathbf{R}}_{22} \boldsymbol{x}_2 - \underline{\mathbf{R}}_{23} \boldsymbol{x}_3\|^2$ in ascending order with its corresponding position, for all possible values of $\boldsymbol{x}_2 \in \boldsymbol{\Omega}_{\mathrm{GQSM}}$. Store the values in **dist2** and **ord2,** respectively.
(9)	$d_{t1} =$ **dist2**(1) + **dist3**(k)
(10)	**for** $m = 1: N_c$,
(11)	$\hat{\boldsymbol{x}}_2 = \boldsymbol{\Omega}_{\mathrm{GQSM}}(\mathbf{ord2}(m),:)$
(12)	Compute and sort the metrics $\mathbf{D}_1^2 = \|\tilde{\boldsymbol{y}}_1 - \underline{\mathbf{R}}_{11} \boldsymbol{x}_1 - \underline{\mathbf{R}}_{12} \hat{\boldsymbol{x}}_2 - \underline{\mathbf{R}}_{13} \hat{\boldsymbol{x}}_3\|^2$ in ascending order with its corresponding position for all possible values of $\boldsymbol{x}_1 \in \boldsymbol{\Omega}_{\mathrm{GQSM}}$. Store the values in **dist1** and **ord1,** respectively.
	Compute $\mathbf{D}_T =$ **dist1**(1) + **dist2**(m) + **dist3**(k)
(13)	**if** $\mathbf{D}_T < \mathbf{D}$
(14)	$d_{t2} =$ **dist1**(1) + **dist2**(m)
(15)	$\mathbf{D} = \mathbf{D}_T$
(16)	$\hat{\boldsymbol{x}}_1 = \boldsymbol{\Omega}_{\mathrm{GQSM}}(\mathbf{ord1}(1),:)$
(17)	$\hat{\boldsymbol{x}}_2 = \boldsymbol{\Omega}_{\mathrm{GQSM}}(\mathbf{ord2}(m),:)$
(18)	$\hat{\boldsymbol{x}}_3 = \boldsymbol{\Omega}_{\mathrm{GQSM}}(\mathbf{ord3}(k),:)$
(19)	$\hat{\boldsymbol{s}}_{\mathrm{GQSM}} = [\hat{\boldsymbol{x}}_1; \hat{\boldsymbol{x}}_2; \hat{\boldsymbol{x}}_3]$
(20)	**end if**
(21)	**if** $m < N_c$
(22)	**if dist2**(m + 1) > d_{t2}
(23)	**break**
(24)	**end if**
(25)	**end if**
(26)	**end for**
(27)	**if** $k < N_c$
(28)	**if dist3**(k + 1) > d_{t1}
(29)	**break**
(30)	**end if**
(31)	**end if**
(32)	**end for**
(33)	Permute $\hat{\boldsymbol{s}}_{\mathrm{GQSM}}$ according to ***order***
(34)	**return** $\hat{\boldsymbol{s}}_{\mathrm{GQSM}}$

VI. Results and Discussion

1. Simulation Results

In this section, results of the proposed scheme are compared in terms of BER performance and complexity. The performance is compared considering a BER of 10^{-3} for the study cases.

Figure 4 shows the performance comparison for a transmission of 8 bpcu with $N_{rx} = 4$ and 4-QAM modulation. It can be observed that the proposed GQSM scheme requires an additional SNR gain of around 1 dB and < 2 dB to obtain a performance similar to the QSM and SM schemes, respectively. In this case, the number of Tx antennas required by SM is $N_{tx} = 64$, QSM requires $N_{tx} = 8$, and GQSM $N_{tx} = 4$, which represents a reduction in N_{tx} of 93% and 50%, respectively.

Figure 5 shows the performance comparison for a transmission of 12 bpcu, $N_{rx} = 4$, and 16-QAM modulation. In this case, the GQSM and SM schemes have a slightly better performance than the QSM scheme for the ML detection. The SM scheme requires $N_{tx} = 256$, QSM requires $N_{tx} = 16$, and GQSM requires $N_{tx} = 4$, which represents a reduction in N_{tx} of 98% and 75%, respectively.

Figure 6 shows the performance comparison for a transmission of 12 bpcu, $N_{rx} = 6$, and 4-QAM modulation. In this case, the number of Tx antennas required by SM is $N_{tx} = 1{,}024$, QSM requires $N_{tx} = 32$, and GQSM requires $N_{tx} = 6$, which represents a reduction in N_{tx} of 99% and 81%, respectively.

Table 6 compares the computational complexity of the proposed detectors. This complexity is measured in terms of the CO used per decoded symbol.

In this comparison, the complexity required to carry out the MMSE SQRD-GQSM algorithm has been included, and it was calculated using the polynomial defined in [14]. In addition, the number of COs required for the algorithms are included in Table 4 and Table 5. The OSIC algorithm has

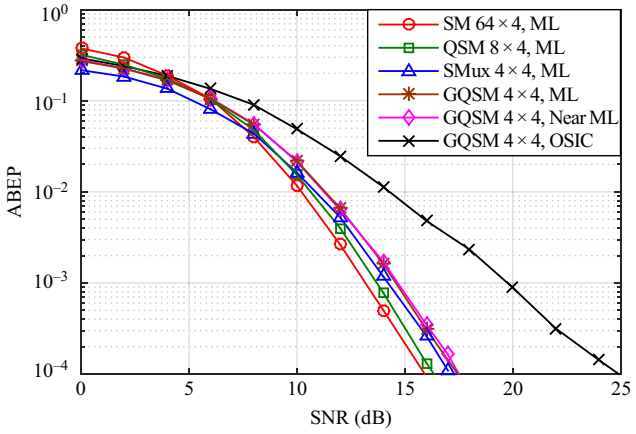

Fig. 4. BER performance versus SNR for 8 bpcu using 4-QAM.

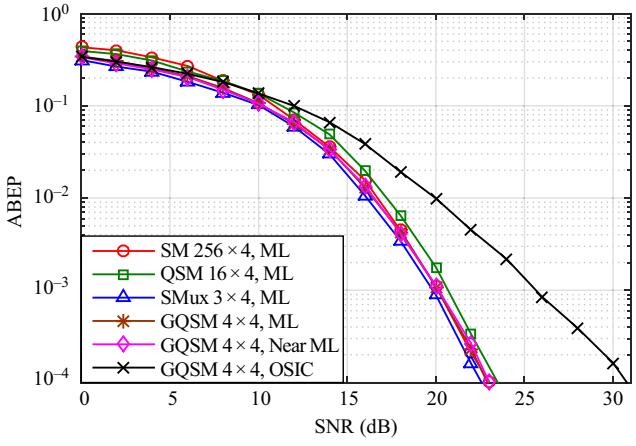

Fig. 5. BER performance versus SNR for 12 bpcu using 16-QAM.

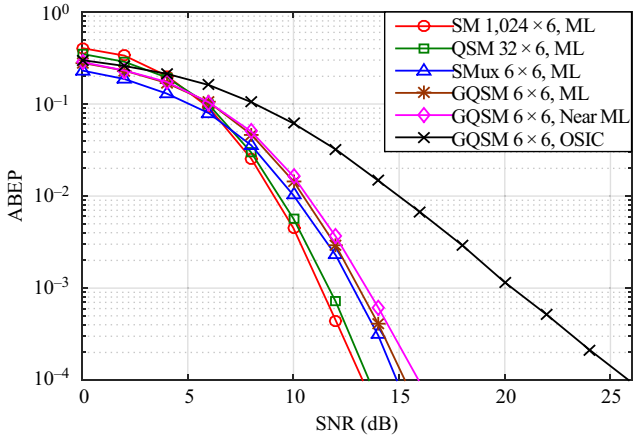

Fig. 6. BER performance versus SNR for 12 bpcu using 4-QAM.

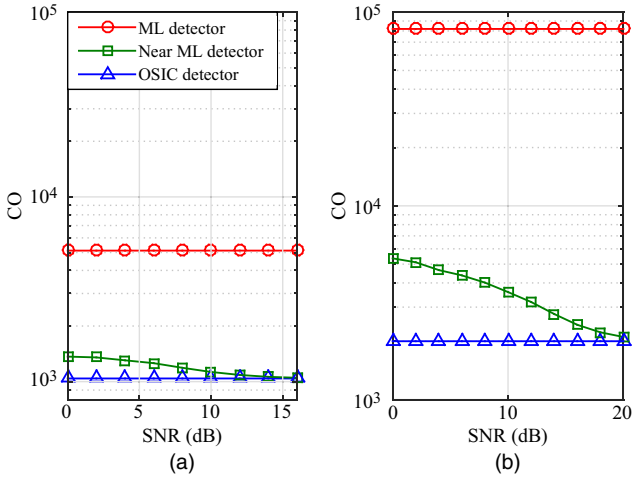

Fig. 7. Variation in the number of complex operations for the OSIC and the near-ML algorithms for the (4 × 4), $n_B = 2$: (a) 8 bpcu and 4-QAM configuration and (b) 12 bpcu and 16-QAM configuration.

https://doi.org/10.4218/etrij.17.0117.0162

Table 6. Complexity comparison in COs for the OSIC and near-ML algorithms.

Detection scheme	8 bpcu (4-QAM) $n_B = 2, N_{rx} = 4$		12 bpcu (16-QAM) $n_B = 2, N_{rx} = 4$		12 bpcu (4-QAM) $n_B = 3, N_{rx} = 6$	
ML	5,120		81,920		147,456	
OSIC	1,039		1,999		2,860	
Near ML	Min	Max	Min	Max	Min	Max
	1,049	1,366	2,046	5,206	2,938	5,146

the lowest complexity. Considering 12 bpcu and 4-QAM, this reduction represents 98%. The near-ML algorithm achieves almost the same reduction in its minimum.

Figure 7 shows a comparison of the variation in the number of COs for ML, near-ML, and OSIC detection algorithms for a (4×4), $n_B = 2$ transmission. (a) Shows the configuration with 8 bpcu and 4-QAM, and (b) shows the configuration with 12 bpcu and 16-QAM. The proposed near-ML algorithm achieves almost the same complexity for SNR values higher than 15 dB and 20 dB, respectively.

2. Discussion

In this study, a perfect CSI was assumed at the Rx; however, the channel estimation requires additional bandwidth, and a larger number of errors can occur in the detection owing to imperfect channel estimation, especially for systems with a large number of Tx antennas. The results obtained in this study show that the SM and some configurations of the QSM scheme have a better BER performance than the proposed GQSM scheme; however, the number of Tx antennas required for the transmission of high data rates may be impractical. Further, the CSI estimation for this system is challenging [19]. The conventional SMux scheme requires a reduced number of Tx antennas and has a slightly better performance compared to the GQSM scheme; however, in this case, its high detection complexity is impractical.

The proposed GQSM scheme inherits advantages and disadvantages of both the QSM and the SMux schemes. The main advantage of the proposed scheme is the flexibility of its system design, which enables the optimization of N_{tx}, performance, and complexity parameters. The proposed scheme can be easily generalized for groups with more than two Tx antennas. While this option reduces the detection complexity of the system, it also reduces the SE. On the other hand, the main disadvantage of the proposed scheme is that the number of RF chains required in the transmitter increases linearly with the number of groups of n_B.

The proposed OSIC algorithm has the lowest complexity; nevertheless, it has important losses in terms of its performance. The proposed Near ML algorithm shows a similar performance to the ML scheme, but with reduced complexity. This complexity is reduced to the OSIC complexity around SNR = 20 dB, which is close to the SNR used for the target BER of 10^{-3}.

VII. Conclusions

In this paper, a spectrally efficient GQSM scheme has been proposed. In the GQSM scheme, the total N_{tx} is divided into small groups of two Tx antennas, where each group uses the QSM technique. Analytical and simulation results show that the ABEP performance of the proposed scheme has losses of < 2 dB when compared to the QSM scheme, but has the advantage of reducing the required N_{tx} by up to 81% for the analyzed cases. Compared with the SMux scheme, the proposed GQSM scheme has roughly the same performance, but with a reduction in detection complexity. In addition, a new efficient algorithm was proposed for the detection of GQSM signals. The proposed Near ML detection architecture performs with a complexity reduction of approximately 90%.

The proposed GQSM scheme introduces many enhancement opportunities that can be considered in future work. For example, i) the incorporation of antenna selection into the grouping process, ii) the effects of imperfect CSI and correlated channels on the system performance, iii) combining the proposed scheme with other techniques such as block diagonalization, which can result in a general performance improvement and/or reduction in complexity detection.

The proposed scheme may be an alternative for future wireless communication systems using the spatial constellations, where space limitations and detection complexity are crucial factors to be considered.

Acknowledgements

This work was supported by the projects PRODEP / SEP UASLP-PTC-598, 2017-2018, the PFCE 2016 and the Sonora Institute of Technology through internal funding for research groups (CAs).

References

[1] R.Y. Mesleh et al., "Spatial Modulation," *IEEE Trans. Veh. Technol.*, vol. 57, no. 4, 2008, pp. 2227–2241.

[2] P.W. Wolniansky et al., "V-BLAST: An Architecture for Realizing Very High Data Rates Over the Rich-Scattering Wireless Channel," in *URSI Int. Symp. Signals, Syst. Electron.*, Pisa, Italy, Oct. 2, 1998, pp. 295–300.

[3] A. Stavridis et al., "An Energy Saving Base Station Employing Spatial Modulation," in *IEEE Int. Workshop Comput. Aided Modeling Des. Commun. Links Netw.*, Barcelona, Spain, Sept. 17–19, 2012, pp. 231–235.

[4] M. Wen et al., "A Low–Complexity Near–ML Differential Spatial Modulation Detector," *IEEE Signal Process. Lett.*, vol. 22, no. 11, 2015, pp. 1834–1838.

[5] F.R. Castillo-Soria et al., "Multiuser MIMO Downlink Transmission Using Block Diagonalization and Generalized Spatial Modulation Techniques," *AEU–Int. J. Electron. Commun.*, vol. 70, no. 9, Sept. 2016, pp. 1228–1234.

[6] C.-X. Wang et al., "Cellular Architecture and Key Technologies for 5G Wireless Communication Networks," *IEEE Commun. Mag.*, vol. 52, no. 2, 2014, pp. 122–130.

[7] R. Mesleh, S.S. Ikki, and H.M. Aggoune, "Quadrature Spatial Modulation," *IEEE Trans. Veh. Technol.*, vol. 64, no. 6, 2015, pp. 2738–2742.

[8] H.-W. Liang et al., "Bi-Space Shift Keying Modulation for MIMO Systems," *IEEE Commun. Lett.*, vol. 16, no. 8, 2012, pp. 1161–1164.

[9] J. Li et al., "Generalized Precoding-Aided Quadrature Spatial Modulation," *IEEE Trans. Veh. Tech.*, vol. 66, no. 2, 2017, pp. 1881–1886.

[10] S. Kim, "Antenna Selection Schemes in Quadrature Spatial Modulation Systems," *ETRI J.*, vol. 38, no. 4, Aug. 2016, pp. 606–611.

[11] A. Younis et al., "Generalised Spatial Modulation," *Conf. Record Asilomar Conf. signals, Syst. Comput.*, Pacific Grove, CA, USA, Nov. 7–10, 2010, pp. 1498–1502.

[12] F.R. Castillo Soria et al., "Improved Detection of SM-SMux Signals for MIMO Channels," *IEEE Latin Am. Trans.*, vol. 13, no. 1, Jan. 2015, pp. 43–47.

[13] M.S. Alouini and A.J. Goldsmith, "A Unified Approach for Calculating Error Rates of Linearly Modulated Signals over Generalized Fading Channels," *IEEE Trans. Commun.*, vol. 47, no. 9, 1999, pp. 1324–1334.

[14] R. Böhnke et al., "MMSE Extension of V-BLAST Based on Sorted QR Decomposition," in *IEEE Veh. Technol. Conf.*, Orlando, FL, USA, Oct. 6-9, 2003, pp. 508–512.

[15] G.H. Golub and C.F. Van Loan, *Matrix Computations*, 3rd edition, Baltimore, MD, USA: John Hopkins University Press, 1996.

[16] M. Mohaisen, H. An, and K. Chang, "Detection Techniques for MIMO Multiplexing: A Comparative Review," *KSII Trans. Internet Inform. Syst.*, vol. 3, no. 6, 2009, pp. 647–666.

[17] B. Kim and K. Choi, "A Very Low Complexity QRD-M Algorithm Based on Limited Tree Search for MIMO Systems," in *IEEE Veh. Technol. Conf.*, Singapore, May 11–14, 2008, pp. 1246–1250.

[18] R. Wang and G. Giannakis, "Aproaching MIMO Channel Capacity with Soft Detection Based on Hard Sphere Decoding," *IEEE Trans.Commun.*, vol. 54, no. 4, 2006, pp. 587–590.

[19] O. Longoria-Gandara and R. Parra-Michel, "Estimation of Correlated MIMO Channels Using Partial Channel State Information and DPSS," *IEEE Trans. Wirel. Commun.*, vol. 10, no. 11, 2011, pp. 3711–3719.

Francisco Rubén Castillo-Soria received his MS in Telecommunications Engineering from IPN-ESIME, Mexico City, in 2004 and his Ph.D. degree in Electronics and Telecommunications from the CICESE Research Center, Ensenada, Mexico, in 2015. Since 2017, he has been a research-professor at Autonomous University of San Luis Potosí, SLP, México. His current research interests include SM, STF coding and MIMO-OFDM.

Joaquín Cortez-González received the MS and the Ph.D. degrees in Electrical Engineering from CINVESTAV-Guadalajara, Mexico, in 2001 and 2008 respectively. He is currently an electrical and electronics engineering professor at the Technologic Institute of Sonora. His research interests include digital communications and digital signal processing.

Raymundo Ramirez-Gutierrez received the MEng. and Ph.D. degrees from the School of Electronic and Electrical Engineering, University of Leeds, Leeds, U.K., in 2009 and 2015, respectively. He is currently a DSP and algorithm researcher at Intel Labs in Guadalajara, Mexico. His research interests lie in the areas of wireless communications and signal processing, coding and modulation, massive MIMO systems, and mmWave technology.

https://doi.org/10.4218/etrij.17.0117.0162

Fermín Marcelo Maciel-Barboza received his MEng degree in communications and electronics engineering, from the Universidad de Colima, Mexico, in 2010 and 2012, respectively. He is currently a professor with the Faculty of Mechanical and Electric Engineering, Universidad de Colima. His research interests include multiuser MIMO communications and cooperative networks.

Leonel Soriano-Equigua received his MS and Ph.D. degrees in Electronics and Telecommunications from the CICESE Research Center, Ensenada, Mexico, in 2000 and 2011, respectively. Since 2000, he has been an assistant professor with the Faculty of Mechanical and Electric Engineering, Universidad de Colima. His area of interest is MIMO communications.